

# Resonance Damping Optimization in 1200V Power Modules with Planar SiC MOSFET Devices for 200 kW Output

Peter S. Ying<sup>1,a\*</sup>, Darwin Tsai<sup>1,b</sup>, Alex Ma<sup>1,c</sup>, George Wu<sup>1,d</sup>, Akira Kamisawa<sup>2,e</sup>,  
Shuichi Miyaoka<sup>2,f</sup>, Nobuo Machida<sup>2,g</sup>, Jimmy Wu<sup>2,h</sup>

<sup>1</sup>Actron Tech Co, 22,Sec.2,Nakan Rd, Luzhu Dis, Taoyuan City, Taiwan ROC

<sup>2</sup>ANJET Corp, 5F.-6, No.308, Zhifu Rd., Zhongshan Dist., Taipei, Taiwan ROC

<sup>a\*</sup>peter\_ying@actron.com.tw, <sup>b</sup>Darwin\_Tsai@actron.com.tw, <sup>c</sup>Alex\_ma@actron.com.tw,  
<sup>d</sup>george\_wu@actron.com.tw, <sup>e</sup>dyx6m@anjet.com, <sup>f</sup>s.miyaoka@anjet.com, <sup>g</sup>n.machida@anjet.com,  
<sup>h</sup>jimmy@anjet.com

**Keywords:** power module, SiC, MOSFET, resonance, damping, planar, trench, power, output.

**Abstract.** Paralleling SiC MOSFETs in high-power modules introduces overvoltage and oscillation risks due to parasitic capacitances and inductances. This study presents a 200 kW EV inverter module co-designed at the device and packaging level to ensure switching reliability under harsh automotive conditions. At 800 V, the planar SiC MOSFET maintained stable gate voltage, while a benchmark trench device module experienced severe ringing and failure. Kelvin-source structures and internal gate resistors mitigated parasitic turn-on, and device-level optimizations—including a 0.5 μm foundry technology, silicide gate, and hexagonal cell layout—improved body-diode performance, together with the channel mobility, blocking voltage, and minimized on-resistance and switching losses. The resulting AEPR25B12C1STJN module demonstrated effective resonance damping, matched the performance of commercial trench module FS03MR12A6MA1B in static and dynamic tests, and achieved 98% AC efficiency with over 200 kW output at 150 °C junction temperature.

## 1. Introduction

Switching transients in SiC MOSFETs can induce unwanted oscillations, or ringing, due to the interaction of parasitic capacitances and inductances. While trench SiC MOSFETs offer performance advantages, they are particularly sensitive to these effects. Ensuring stable and reliable switching requires effective damping and careful device-module co-design[1][7]. This study presents the development of a 200 kW planar SiC power module for EV traction inverters, emphasizing resonance-damped gating, low on-resistance, and device-level optimization, especially in the  $R_g$  and  $V_t$ [4]. Improvements in device design, foundry technology, and cell layout enhanced blocking voltage, oxide reliability, and minimized switching losses. The resulting 6-in-1 AEPR25B12C1STJN module avoids ringing damage, achieves performance comparable to a commercial trench module (FS03MR12A6MA1B), and was validated via Dyno testing for high-reliability EV powertrain application.

## 2. Device Samples for 1200V Planar and Trench SiC MOSFET Modules

Paralleling SiC MOSFETs in high-power modules introduces overvoltage and oscillation risks due to parasitic inductance. To evaluate switching behavior, 1200V planar and trench SiC MOSFETs were compared. The trench device was sourced from a 4th-generation commercial product [2], while the planar device was custom-fabricated using foundry technology [3]. Figure 1 presents the cross-sectional SEM and cell layouts, and Table 1 summarizes key datasheet parameters.



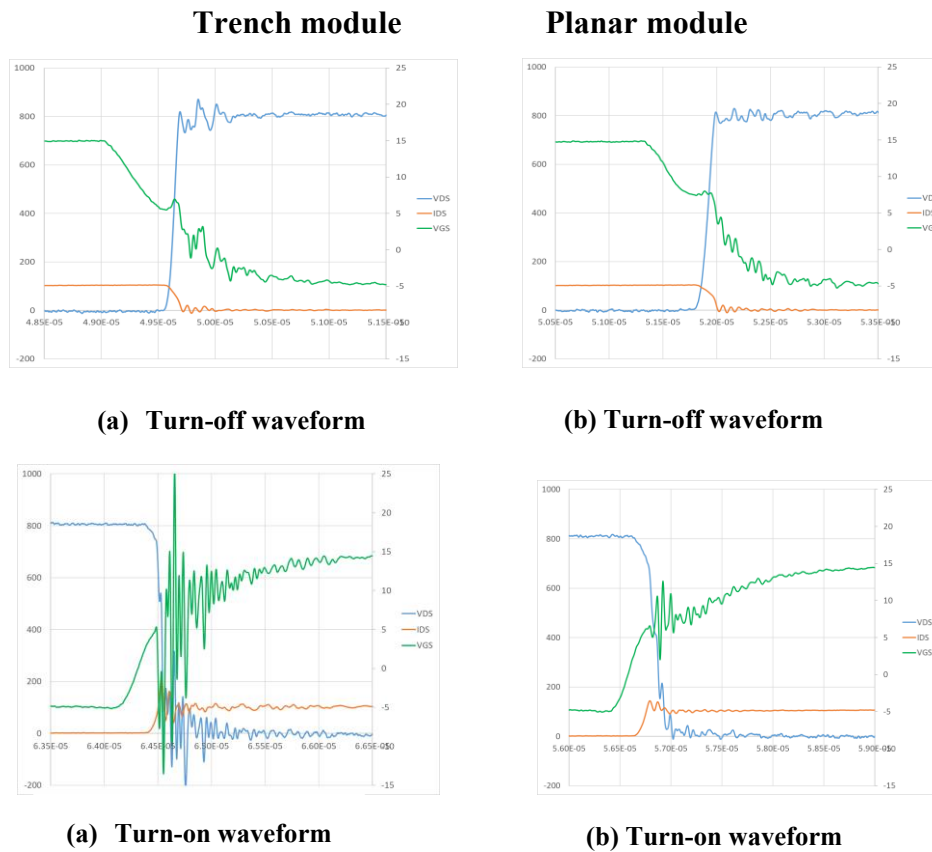


Fig. 2. Waveform comparison of trench and planar modules.

Table 2. Dynamics characteristics of trench and planar module.

ITEMS	PARAMETERS	TEST CONDITION	TRENCH MODULE	PLANAR MODULE	UNIT
TURN ON	Vgs (MAX)	HV <sub>dc</sub> =800V, I <sub>d</sub> =100A V <sub>gs</sub> =-5V to 15V, R <sub>g,on</sub> = 5.1ohm R <sub>g,off</sub> = 5.1ohm	12.3	24.9	V
	Vgs (MIN)		2	-11.7	
TURN OFF	Vgs (MAX)		3.7	2.9	V
	Vgs (MIN)		-0.7	-3.3	

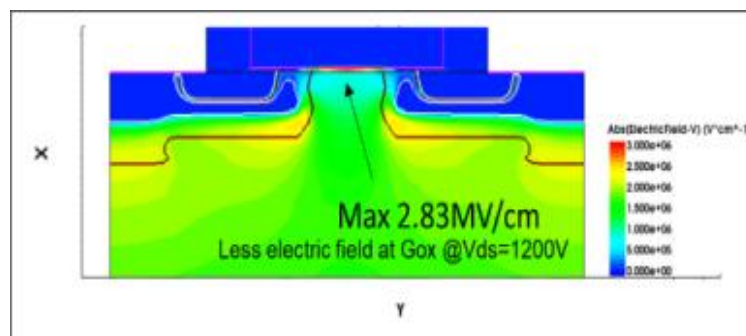


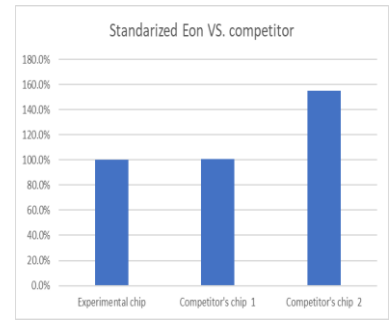
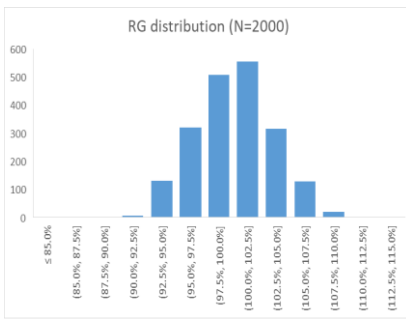
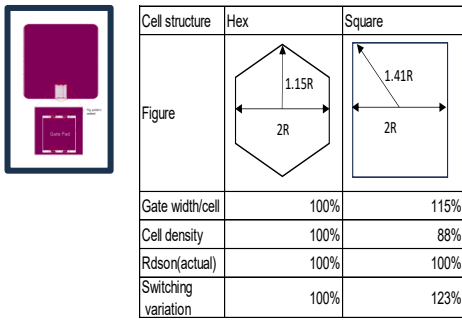
Fig. 3. TCAD simulation showed junction profiles enable E-field at Gox @V<sub>ds</sub> =1200V.

#### 4. Customization of Planar 1200V SiC MOSFET with Foundry Technology

The planar device was optimized for high-performance switching. Enhancements included a Kelvin source structure, internal gate resistance, and improved body diode design to support reverse recovery without an external Schottky Barrier Diode. TCAD simulation (Figure 3) confirmed reduced electric field stress (<2.83 MV/cm) at 1200 V V<sub>ds</sub>.

Key foundry process steps included dry oxidation with NO anneal for high-quality gate oxide, high-temperature ion implantation and >1400°C anneal to reduce interface trap density (Dit), Short channel (0.5 μm) to reduce Ron, and optimized doping profiles in N+/N- drift and P-well/P-body regions.

Layout enhancements (Figure 4), including hexagonal cell structures, silicide-gate integration, optimized gate runners, and Rg-spreading control (Figure 5), resulted in improved thermal performance and reduced switching losses. Benchmark evaluations further verified the reduction in Eon and demonstrated robust high-temperature performance.



\*Standard Eon = Eon/Ciss

Fig. 4. Hexagonal & cellular layout for uniform current.

Fig. 5. 10% Rg control.

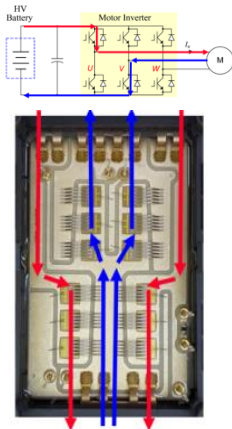
Fig. 6. Less or equal Eon with Rg Spreading.

Figure 6. showed the equal or less Eon loss benchmarked with two competitors. The key performance metrics is then to achieve greater than 1400V Breakdown Voltage, less than 10 mΩ·cm<sup>2</sup> area specific resistance, achieved gate oxide reliability of >10<sup>6</sup> hrs at 25°C with the <2.5V Vf of body diode. Low Qgd <50 nC is for fast switching purpose.

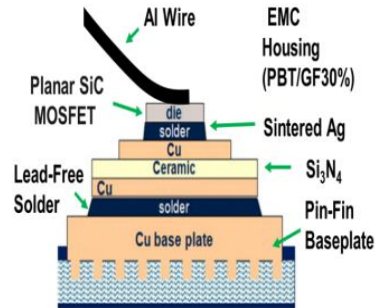
### 5. 200 kW Power Module Design for EV Traction Inverter

A holistic design strategy was applied to the 200-kW half-bridge module, combining a customized planar SiC MOSFET with a gate-drive scheme tuned for resonance damping. The resulting 1200V/400A module focused on minimizing parasitic capacitance and inductance, improving thermal performance, and maintaining layout symmetry. Key features include a high-density, low-inductance structure; Cu-clip and Al-wire bonding for enhanced electrical and thermal efficiency; and a pin-fin baseplate on a Si<sub>3</sub>N<sub>4</sub> AMB substrate for direct liquid cooling. The design incorporates an integrated NTC sensor and press-fit terminals (Figure 8) and meets UL 94 V-0 and CTI > 200 requirements (Figure 9).

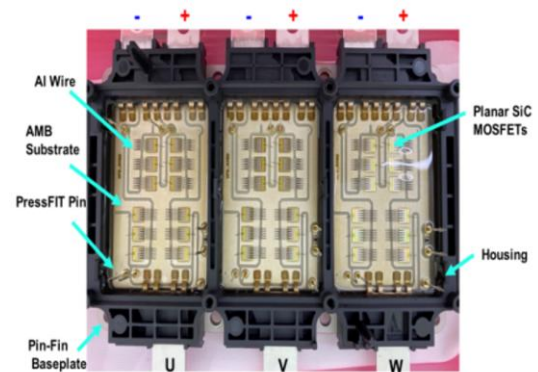
The symmetric current layout (Figure 7) ensures uniform current sharing and thermal distribution, supporting high-power operation. The improved planar MOSFET body-diode performance eliminates the need for an external SBD. The module structure employs lead-free interconnects, a liquid-cooled pin-fin baseplate, and a Si<sub>3</sub>N<sub>4</sub> AMB substrate, with press-fit contacts and a 150 °C-rated NTC enabling flexible integration into EV inverter systems.



**Fig. 7.** Symmetric current layout.



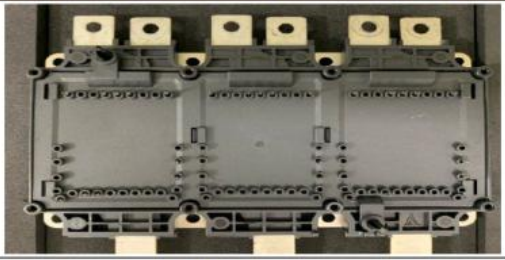

**Fig. 8.** Schematic of power module design.



**Fig. 9.** Top view & outfit of the Actron power module.

Figure 9 shows the top view and the outfit of the power module. The power module frame has passed rigorous vertical burning test UL 94 V-0, and insulation resistance of a material Comparative Tracking Index CTI > 200. This module has qualified according to AQG 324 with KS pin available and Negative Temperature Control (NTC) integrated.

## 6. Benchmark against Commercial Trench Module

ATC	Ixx
	
<ul style="list-style-type: none"> <li>• AEPR25B12C1STJN</li> <li>• With SiC Automotive MOSFET</li> <li>• Six-pack module 1200V/400A</li> </ul>	<ul style="list-style-type: none"> <li>• FS03MR12A6MA1B</li> <li>• HybridPACK™ Drive module with CoolSiC™ Automotive MOSFET</li> <li>• Six-pack module 1200V/400A</li> </ul>

**Fig. 10.** AEPR25B12C1STJN benchmark with FS03MR12A6MA1B.

The AEPR25B12C1STJN planar module (same 216 mm<sup>2</sup> chip area with competition) was benchmarked against the FS03MR12A6MA1B trench module [5]. (Figure 10) DPT at HVDC = 600 V, Id = 400 A with Rg,on / Rg,off = 5.1 Ω / 5.1 Ω showed comparable switching behavior. Planar SiC MOSFETs has lower Cgd and weaker Miller coupling with stable inversion channel under fast switching. It can safely operate with a lower Vt without risking false triggering therefore it is naturally more immune to dV/dt noise showing in Figure 11.

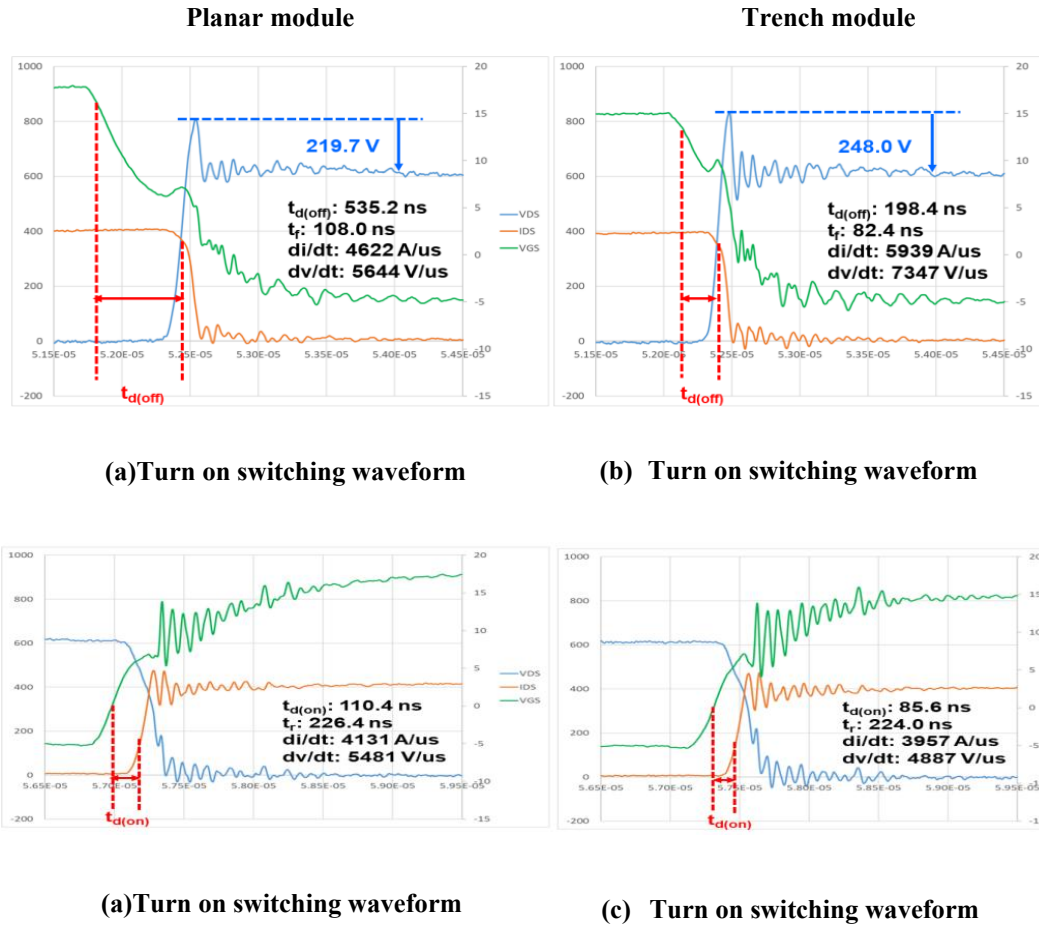


Fig. 11. Waveform comparison between planar and trench Module.

Table 3. Static and dynamic test comparison Between Planar and trench module.

Static Characteristics	T <sub>J</sub> °C	I <sub>gss</sub> nA	I <sub>dss</sub> μA	V <sub>th</sub> V	R <sub>DS(ON)</sub> mΩ	Q <sub>g</sub> μC	C <sub>iss</sub> nF	C <sub>oss</sub> nF	C <sub>riss</sub> nF	V <sub>SD</sub> V
ATC	25	1.62	0.08	2.52	2.04	1.87	45.1	2.02	0.16	5.16
I <sub>xx</sub>		0.86	0.03	4.56	2.83	1.23	41.7	1.73	0.11	4.41
I <sub>xx</sub> Datasheet		400	100	4.40	2.75	1.32	42.6	1.86	0.17	4.42

Static Characteristics	T <sub>J</sub> °C	I <sub>gss</sub> nA	I <sub>dss</sub> μA	V <sub>th</sub> V	R <sub>DS(ON)</sub> mΩ	Q <sub>g</sub> μC	C <sub>iss</sub> nF	C <sub>oss</sub> nF	C <sub>riss</sub> nF	V <sub>SD</sub> V
ATC	150	-	34.0	1.86	3.14	-	-	-	-	4.44
I <sub>xx</sub>		-	0.11	3.81	4.78	-	-	-	-	4.08
I <sub>xx</sub> Datasheet		-	-	-	4.55	-	-	-	-	-

Dynamic Characteristics	T <sub>J</sub> °C	t <sub>d(on)</sub> ns	t <sub>r</sub> ns	E <sub>on</sub> mJ	di/dt kA/μs	t <sub>d(off)</sub> ns	t <sub>f</sub> ns	E <sub>off</sub> mJ	dv/dt kV/μs	I <sub>RM</sub> A	t <sub>rr</sub> ns	Q <sub>rr</sub> μC	E <sub>rec</sub> mJ
ATC	25	110	226	18.1	4.1	535	108	26.0	5.6	67	52.0	2.2	0.53
I <sub>xx</sub>		86	224	21.6	4.0	198	82	22.8	7.3	74	54.4	2.5	0.63
I <sub>xx</sub> Datasheet		77	79	19.5	4.0	263	64	17.6	7.3	165	-	11.2	1.4

Dynamic Characteristics	T <sub>J</sub> °C	t <sub>d(on)</sub> ns	t <sub>r</sub> ns	E <sub>on</sub> mJ	di/dt kA/μs	t <sub>d(off)</sub> ns	t <sub>f</sub> ns	E <sub>off</sub> mJ	dv/dt kV/μs	I <sub>RM</sub> A	t <sub>rr</sub> ns	Q <sub>rr</sub> μC	E <sub>rec</sub> mJ
ATC	150	82	185	17.9	4.4	641	111	28.2	5.3	149	74.4	6.5	1.83
I <sub>xx</sub>		52	188	22.1	4.4	231	84	23.2	7.1	173	80.0	7.5	2.33
I <sub>xx</sub> Datasheet		59	69	20.2	4.6	294	65	18.2	7.1	309	-	19.3	4.7

V<sub>GS</sub> = -5V/+15V at IFX datasheet

Commercial trench SiC MOSFETs provide higher channel density and current capability, enabling current peaks of several hundred amperes per switch during motor transients or regenerative braking in >100-kW EV inverter operation. As shown in Figure 11, both devices exhibit comparable switching behavior; however, the trench module produces a higher turn-on surge voltage (248 V) than the planar module (219.7 V), reflecting its greater susceptibility to voltage overshoot.

This behavior is linked to an inherent structural disadvantage of trench devices: the vertical gate geometry and tight cell pitch significantly increase the gate-to-drain capacitance  $C_{gd}$  and higher Miller coupling, making the device highly sensitive to  $dv/dt$  induced parasitic turn-on. Under these conditions, the complementary switch in the half-bridge can inadvertently conduct, creating a shoot-through path that threatens module reliability.

To prevent this, the trench MOSFET must operate with a substantially higher threshold voltage 4.56 V as shown in Table 3, to provide sufficient immunity against noise-induced gate excitation, premature channel formation, and field-stress-induced oxide degradation at the trench corners. In contrast, planar SiC MOSFETs inherently exhibit lower  $C_{gd}$ , weaker gate-drain coupling, and a more uniform electric-field distribution, enabling them to operate safely with a lower  $V_{th}$  of 2.52 V while still achieving comparable switching energy loss and overall efficiency.

## 7. Dyno Test and System-Level Efficiency

As summarized in table 4, Dyno testing conducted at 800 V and 1000 rpm confirmed that both the planar and trench SiC MOSFET modules delivered 220 kW AC output at 2000 Nm torque with a comparable inverter efficiency of 98%. The measured torque, rotational speed, and output power demonstrate that both module technologies meet the performance targets under full-load operating conditions.

However, the competitor's trench-based module exhibited a slightly higher junction temperature, indicating that the planar-based design provides marginally superior thermal conduction. This improved thermal behavior suggests additional margin for sustaining higher output capability or enhanced reliability under real-world EV operating conditions[6].

**Table 4.** Dyno test comparison between planar and trench module.

Operation condition:  $V_{GS}$ : -4V/15V,  $R_{g,on}$ : 5  $\Omega$ ,  $R_{g,off}$ : 5  $\Omega$

Cooler temp. (°C)	Module	Operation mode	Speed (rpm)	Torque (Nm)	HVDC (V)	DC Current (A)	DC Power (W)	AC Voltage (V)	AC Current ( $A_{rms}$ )	AC_Pow (kW)	MCU_eff (%)	$T_j$ (°C)
65	Ixx	Low torque	1000	1151	799.9	158.77	126.9	404.2	197.7	124.5	98.03	73.96
	ATC		1000	1142	799.9	157.67	126.1	391	197.9	123.4	97.9	75.12
	Ixx	High torque	1000	2040.8	799.5	285.66	228.3	489.3	339.4	223.1	97.69	101.8
	ATC		1000	2009	799.52	282.72	226	475.6	332.9	220.7	97.6	99.2

## 8. Summary and Conclusions

This study presents a resonance-damping strategy to ensure safe and reliable operation of a 200-kW EV-inverter power module. Double-pulse testing showed that the planar SiC MOSFET module maintained stable gate behavior, whereas the benchmark trench module exhibited severe ringing and catastrophic failure at 800 V, 100 A. Consequently, the planar architecture—enhanced with a Kelvin-source layout and integrated gate resistance—was selected for further development.

A custom 1200V planar SiC MOSFET module was designed and validated through simulation, Double Pulse Testing, and system-level testing, featuring optimized junction doping to balance reverse-recovery softness, conduction performance, and power density.

The device achieved >1400 V blocking capability, specific  $R_{on} < 10 \text{ m}\Omega \cdot \text{cm}^2$ , gate-oxide lifetime >10<sup>6</sup> hours, body-diode  $V_f < 2.5 \text{ V}$ , and  $Q_{gd} < 50 \text{ nC}$ . The AEPR25B12C1STJN module employed a high-reliability packaging platform with Cu-clip and Al-wire bonding, a Si<sub>3</sub>N<sub>4</sub> AMB pin-fin baseplate for liquid cooling, an NTC rated to 150 °C, and press-fit terminals.

System-level evaluation confirmed superior switching performance, thermal robustness, and efficiency compared with commercial trench modules. The design passed UL 94 V-0 and insulation tests (CTI > 200) and qualified under AQG 324 standards. Benchmarking against the FS03MR12A6MA1B commercial trench module demonstrated reduced ringing, improved damping, lower  $R_{ds(on)}$ , reduced  $E_{on}/E_{off}$  at high temperatures, and enhanced thermal stability. Dynamometer testing at 800 V and 1000 rpm further verified 220 kW AC output at 2000 Nm torque with 98% inverter efficiency and a slight thermal advantage under real-world conditions.

## References

- [1] IET Power Electronics, Vol 15, Issue 11, Pages 989-1109 (2022).
- [2] <https://www.rohm.com/products/sic-power-devices/sic-mosfet/sct4013dr-product>.
- [3] <https://www.xfab.com/technology/sic-gan#c2574>.
- [4] Semicond. Technol. 43(3), 181–187 (2018).
- [5] <https://www.alldatasheet.com/datasheet/INFINEON/FS03MR12A6MA1LB>.
- [6] B.J. Baliga, “Fundamentals of Power Semiconductor Devices”, Springer-Scientific Press, New York, 2008.
- [7] Saeed Anwar, Zhiqiang (Jack) Wang, and Madhu Chinthavali, “Characterization and Comparison of Trench and Planar Silicon Carbide (SiC) MOSFET at Different Temperatures” 2018 IEEE Transportation Electrification Conference and Expo (ITEC) 13-15 June 2018.